J. Membrane Biol. 159, 71–82 (1997)

The Journal of
Membrane
Biology

Voltage-Dependent Anion Channel of *Arabidopsis* Hypocotyls: Nucleotide Regulation and Pharmacological Properties

S. Thomine, J. Guern, H. Barbier-Brygoo

Institut des Sciences Végétales, Centre National de la Recherche Scientifique, Bât. 22, Avenue de la Terrasse, F-91198 Gif-sur-Yvette Cedex, France

Received: 26 December 1996/Revised: 21 March 1997

Abstract. Plasma membrane anion channels are thought to play important roles in osmoregulation and signal transduction in higher plant cells. Knowledge of their pharmacology and regulation is of importance to unravel their physiological functions. In this study, we explore the pharmacological properties and the nucleotide regulation of the voltage-dependent anion channel of *Arabidopsis* hypocotyls. The pharmacological profile of this channel is characterized by a low sensitivity to most anion channel blockers. It is inhibited by niflumic acid with an IC_{50} of 80 μM, but poorly sensitive to IAA-94 and NPPB and insensitive to 9-AC and DIDS. Nucleotides alter the amplitude, the kinetics and the voltage-dependence of the channel. The main effect of nucleotides is a shift of the voltage-dependent gate of the channel toward depolarized potentials leading to a strong reduction of the current amplitude. This regulation does not require ATP hydrolysis as nonhydrolyzable ATP analogues—AMPPNP and ATPγS—also regulate the anion current. This suggests that a nucleotide binding site is involved in the regulation. The study of the properties of this putative nucleotide binding site reveals that (i) ATP regulates the channel with an EC_{50} of 0.7 mM, (ii) adenyl nucleotides modulate the channel with the following order of effectiveness: ATP > ADP ⩾ AMP, and (iii) thiophosphate nucleotide analogues are the most potent agonists with EC_{50} in the range of 80 μM. The hypothesis that this regulation may couple the electrical properties of the membrane with the metabolic status of the cell is discussed.

Key words: Anion channel — *Arabidopsis* — Inhibitors — Niflumic acid — Nucleotide — Plant

Correspondence to: S. Thomine

Introduction

Recent studies reveal important roles for plasma membrane anion channels in plant cell osmoregulation and signal transduction (Tyerman, 1992). The study of their pharmacological properties as well as the knowledge of their regulations represent two means that can help in the identification of their physiological functions. The use of channel antagonists is helpful to evaluate the contribution of a channel in integrated physiological processes. In guard cells, for instance, blockers of the slow anion channel prevent the closure of stomata pointing to a major role of anion channels in electrolyte efflux from these cells that leads to stomatal closure (Schroeder, Schmidt & Sheaffer, 1993; Schwartz et al., 1995). Blockers have also been used to demonstrate the involvement of anion channels in the transduction of various signals (Ward, Pei & Schroeder, 1995). Anthracene-9-carboxylic acid (9-AC), an anion channel blocker, is a potent inhibitor of plant cell responses to fungal elicitors (Ebel & Cosio, 1994) suggesting an important role of anion channels in elicitor signal transduction. More recently, an anion channel of *Arabidopsis* hypocotyl cells was shown to be responsible for the depolarization induced by blue light in this organ (Cho & Spalding, 1996) and thus is likely to participate in the transduction of blue light responses.

The knowledge of the factors that regulate a particular channel can also provide some hints concerning its function. In the case of anion channels, the study of their regulation and especially of their downregulation is of major interest, because the opening of anion channels dramatically perturbs the electrical equilibrium of the plant cell. Indeed, as the equilibrium potential for anions resides far from the resting potential of the plant cell plasma membrane, the opening of anion channels leads to a depolarization and/or to a massive salt efflux. This can be used by plant cells either to transduce signals or

to regulate their osmotic pressure but has to be prevented in cells at rest. Examples showing that anion channels are subjected to strong regulation and that a channel type is often the object of multiple regulations have recently been described. The slow anion channel of guard cells is regulated by both intracellular calcium (Schroeder & Hagiwara, 1989) and phosphorylation processes (Schmidt et al., 1995). This channel is activated by a rise of $[Ca^{2+}]_{in}$ from 10 nM to 1500 nM (Schroeder & Hagiwara, 1989). When $[Ca^{2+}]_{in}$ is set to 240 nM, a concentration that allows the activation of anion currents, the channel can be upregulated by protein phosphatase inhibitors and downregulated if phosphorylation is inhibited either by depleting intracellular ATP or using protein kinase inhibitors (Schmidt et al., 1995). Even more complex is the regulation of the rapid anion channel of guard cells (GCAC1). An increase in intracellular calcium as well as the presence of nucleotides are required to activate the current (Hedrich, Busch & Raschke, 1990; Schulz-Lessdorf, Lohse & Hedrich, 1996). In the presence of calcium and nucleotides, the current that activates is strongly voltage-dependent with a threshold for activation around −80 mV which is far from the usual resting potential of plant cells. A third level of regulation is achieved by extracellular anionic ligands such as auxin and malate. These two molecules are able to shift the voltage-dependence of the current so that the threshold for activation becomes more hyperpolarized and closer to the resting potential of the guard cells (Hedrich & Marten, 1993; Marten, Lohse & Hedrich, 1991). Thus, several levels of regulation are overlayed to control the opening of GCAC1.

A similar scheme seems to be valid also for the voltage-dependent anion channel of *Arabidopsis* hypocotyls (Thomine et al., 1995). The activation of the current after establishment of the whole-cell configuration and its subsequent rundown suggests that cytoplasmic factors are necessary to maintain channel activity. The mechanism of this regulation is not yet understood and the activating factors remain to be identified. An additional level of control that involves ATP has been described (Thomine et al., 1995). Intracellular ATP increases change the voltage range in which the channel is active so that larger depolarizations are required to activate it. However, the question remained whether ATP regulates the channel via phosphorylation events as described for the tobacco cell anion channel (Zimmermann et al., 1994) and the S-type anion channel of guard cells (Schmidt et al.,1995) or whether it operates via a nucleotide binding site as described for the R-type anion channel of guard cells (Hedrich et al., 1990) and a class of animal potassium channels (Ashcroft, 1988).

In this work, we describe novel properties of the voltage-dependent anion channel of hypocotyl epidermal cells in terms of sensitivity to anion channel blockers and of regulation by nucleotides. We show that this channel is efficiently blocked by niflumic acid but is insensitive to both 9-AC and DIDS and poorly sensitive to IAA-94 and NPPB which are potent inhibitors of guard cell anion channels (Marten et al., 1992, 1993; Schroeder et al., 1993; Schwartz et al., 1995). We provide arguments that the regulation of the channel by ATP reflects the interaction of ATP with a nucleotide binding site rather than its use as a substrate for kinases and describe the specificity of the nucleotide binding site. We also provide arguments that the nucleotides act mainly, if not only, by shifting the voltage gate of the channel towards depolarized potential. This channel thus displays original properties in terms of nucleotide-dependent regulation and pharmacological sensitivity when compared with the other anion channels already described in higher plant cells.

Materials and Methods

Plant Material and Protoplast Isolation

Seedlings (*Arabidopsis thaliana* ecotype Columbia), were grown on a medium containing (in mM); 5 KNO_3, 2.5 K_2HPO_4/KH_2PO_4, pH 6, 2 $MgSO_4$, 1 $Ca(NO_3)_2$, 1 Mes, and 50 μM FeEDTA, Murashige and Skoog microelements (Murashige & Skoog, 1962), 10 g/L sucrose and 7 g/L agar. Culture conditions were 21°C, with a 16-hr day length at lighting levels of 120 $\mu E\ m^{-2}\ sec^{-1}$ with neon tubes (a combination of Mazdafluor Blanc Industrie and Mazdafluor Prestiflux). Seedlings aged of 9 to 12 days were used for electrophysiological investigations. Hypocotyls were excised from 30 to 40 seedlings and protoplasts were isolated according to Elzenga (1991) as described in Thomine et al. (1995).

Electrophysiological Investigations

Whole-cell patch-clamp experiments were performed as described by Hamill et al. (1981) using an Axon 200A amplifier (Axon Instruments, Foster City, CA). During measurements, freshly isolated epidermal protoplasts from *Arabidopsis* hypocotyls were maintained in bathing medium (in mM): 50 $CaCl_2$, 5 $MgCl_2$, 10 Mes-Tris, pH 5.6. The pipettes were filled (in mM) with 150 KCl, 2 $MgCl_2$, 2 EGTA, 1.8 $CaCl_2$, 10 Tris-Mes, pH 7.2, supplemented with nucleotides as indicated. The osmolalities of both solutions were adjusted to 450 mOsmol with mannitol using a Wescor 5500 vapor pressure osmometer (Wescor, Logan, Utah). Gigaohm resistance seals (1–10 GΩ) between pipettes (pipette resistance 1 to5 MΩ) coated with Sylgard (General Electric, New York) pulled from Kimax-51 capillaries (Kimble Glass, Owens, IL) and protoplast membranes were obtained with gentle suction leading to whole-cell configuration. The liquid junction potential was measured according to Neher (1992). All the potentials given have been corrected for a junction potential of +4 mV.

Application of voltage programs and handling of the data were performed using a Digidata 1200 interface and patch-clamp software pClamp 6.0.2. with Clampex and Clampfit (Axon Instruments, Foster City, CA). The filter frequency was set to 2 kHz. Capacitive transients were corrected during the patch-clamp experiments, but very fast transients (≤1 msec) could not always be completely eliminated (*see* Figs. 2 and 3). For the pharmacological tests, pipettes yielding rather high

access resistance in the range of 10 MΩ were used to prevent rapid rundown of the anion current. In contrast, in the experiments testing the effect of intracellular nucleotides, large pipettes leading to low access resistance seals (2–5 MΩ) were used to achieve fast and efficient perfusion of the cytoplasm. The series resistance was compensated to more than 85% when necessary. No leak substraction was applied on any of the recordings. In some cases, the currents are expressed as current density ($\mu A/cm^2$) assuming that the membrane capacity is 1 $\mu F/cm^2$. Unless otherwise indicated, figures are shown for one representative protoplast, and statistics are given as mean ± SD (*n* indicates the number of protoplasts tested).

Inhibitors

The anion channel blockers 9-AC (Anthracene-9-carboxylic acid), DIDS (4,4′-diisothiocyanato-stilbene-2-2′-disulfonic acid) and niflumic acid were purchased from Sigma-Aldrich (St. Louis, MO). IAA-94 (R(+)-methylindazone; indanyloxyacetic acid 94) was purchased from RBI (Natick, MD). NPPB (5-nitro-2-(3-phenylpropylamino)benzoic acid) was purchased from Tocris Cookson (St. Louis, MO). They were prepared as stock solutions in ethanol so that the final concentration of ethanol in the bath solution never exceeded 1%, a concentration which had no effect on the anion current. 9-AC was also tested when initially dissolved in 1 M NaOH, in this case, the final concentration of NaOH was 0.5 mM and it did not change the pH of the external bath solution.

Nucleotides

All the nucleotides were purchased from Sigma (St. Louis, MO). Adenosine-5′-trisphosphate (ATP) was tested either as a Mg^{2+} chelate or as a K^+ salt (as indicated in the results and in the figure legends). Adenosine-5′-phosphate (AMP) and adenosine-5′-diphosphate (ADP) were tested as K^+ salts. Guanosine-5′-triphosphate (GTP), 5′-adenylylimidodiphosphate (AMPPNP), adenosine-5′-O-(3-thiotriphosphate) (ATPγS), adenosine-5′-O-(-thiodiphosphate) (ADPβS), guanosine-5′-O-(3-thiotriphosphate) (GTPγS) and guanosine-5′-O-(-thiodiphosphate) (GDPβS) were tested as Li^+ salts. It was checked that 10 mM Li^+ had no effect by itself on the voltage dependence of the anion current.

Determination of Relative Open Probability

The relative open probability was measured in the whole-cell configuration using a two step voltage protocol. The membrane potential was first stepped from a holding potential of −184 mV to various depolarized voltages (V_m) to activate the channels. Then, it was stepped back always to the same potential E_{hold} (usually −184 mV) at which the driving force for chloride is high. We measured the current at the very beginning of this second pulse before the deactivation, when the open probability can still be assumed to be that which prevailed at the V_m imposed during the preceding depolarizing step. This current can be written as $I_{tail} = N \cdot g \cdot (E_{hold} - E_{Cl}) \cdot P_o$ where *N*, the total number of active channels, *g* the single channel conductance and $(E_{hold} - E_{Cl})$ the driving force for Cl are constant, and P_o is the open probability of the channel at the end of the first pulse. Thus I_{tail} is proportional to the open probability of the channel and the ratio $I_{tail}/I_{tail\ max}$ represents the relative open probability. The variations of the relative open probability of the channel with the potential were then fitted using the Boltzmann equation:

$$P_o = 1/[1 + \exp[(z_g e/kT) \cdot (V_m - V_{1/2})]]$$

where *e* is the elementary charge, *k* the Boltzmann constant and *T* the absolute temperature (293 K); V_m stands for membrane potential and z_g, the gating charge, and $V_{1/2}$, the half activation potential, are characteristic parameters of the channel.

Modeling of the *I-V* Curve of the Anion Current

The experimental *I-V* data have been fitted with a calculated function as $I(V_m) = I_{GHK}(V_m) \cdot P_o(V_m)$. I_{GHK} represents the current calculated according to the Goldman-Hodgkin-Katz (GHK) equation (Hille, 1992). The permeability coefficient of the GHK equation has been used as an adjustable parameter to fit the calculated function to the experimental data. The voltage dependence of the open probability (P_o) has been calculated from the Boltzmann equation using the parameters from the fitting of the experimentally determined normalized open probability (*see* previous section). The rectification of the current between the peak potential and 0 mV was fitted as a voltage dependent reduction of the current by an additional Boltzmann function with a gating charge of 0.7 and a potential of half inhibition −115 mV.

Results

Niflumic Acid, IAA-94 and NPPB Interact with Hypocotyl Voltage-dependent Anion Channels

Various anion channel blockers were tested in the whole-cell patch-clamp configuration on protoplasts from epidermal cells of *Arabidopsis* hypocotyls. When the current amplitude had reached a stable value for more than one minute, the inhibitors were applied in the extracellular medium using a local perfusion pipette. Local perfusion around a protoplast of either 100 μM DIDS ($n = 3$) or 9-AC ($n = 7$), potent inhibitors of guard cell anion channels, did not induce any significant inhibition of the voltage-dependent anion current on a 5-to-10-min time scale (*data not shown*, in Fig. 1*B*, 9-AC was simply injected in the bath solution). We also investigated whether 9-AC or DIDS could act on the cytoplasmic side of the membrane. When 9-AC and DIDS were added at the concentration of 100 μM in the patch pipette, neither did they prevent the activation of the current nor did they induce an obvious reduction in the current amplitude.

Figure 1*A* illustrates the inhibition of the anion current by 0.5 mM niflumic acid. The peak amplitude was reduced by 87% and the peak potential was shifted by 10 mV toward hyperpolarized potentials. Figure 1*B* displays the intensity of the current as a function of time after establishment of the whole-cell configuration. It shows that, whereas addition of 0.1 mM 9-AC in the external solution had no significant effect, the onset of the local perfusion system containing 0.1 mM niflumic acid induced immediate inhibition. Steady-state inhibition by niflumic acid was reached within 20 sec (time between two test protocols) after the onset of the perfusion. When the local perfusion was stopped, the current came back to the control value within 30 sec to 1 min.

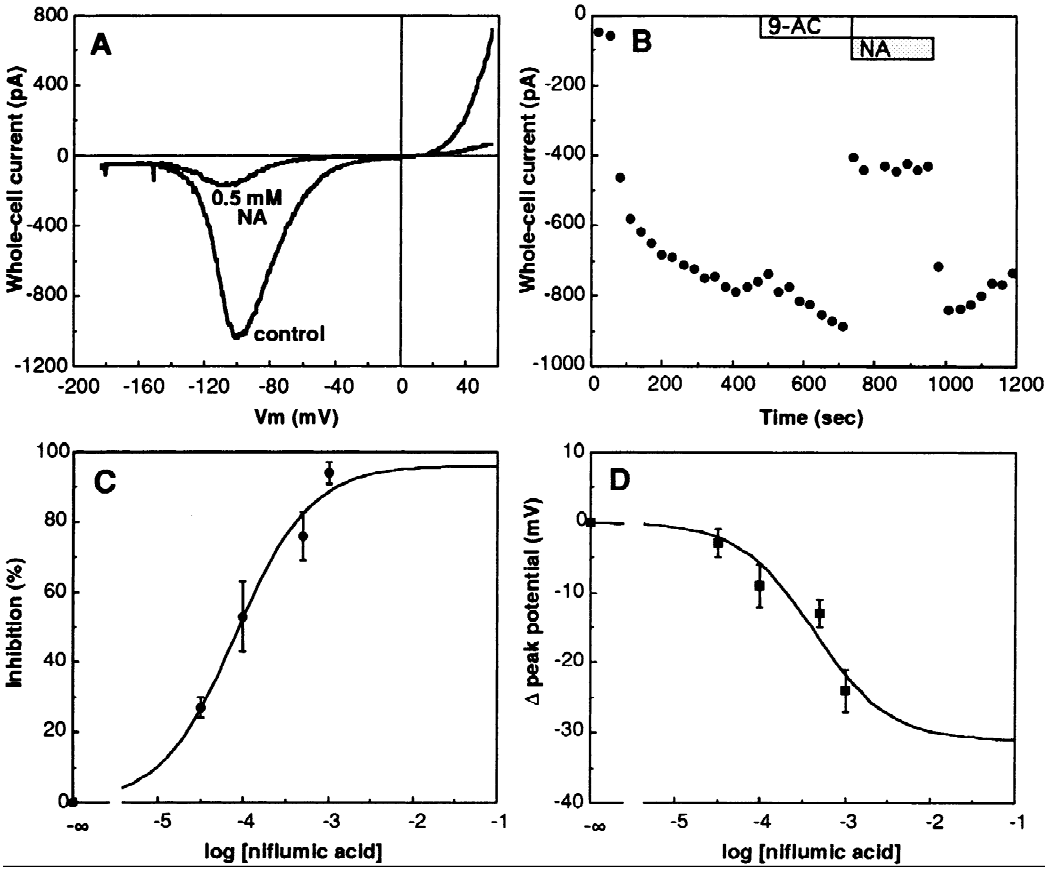

Fig. 1. Effects of niflumic acid (NA) on the voltage-dependent anion current of hypocotyl cells. Whole-cell currents were measured on hypocotyl epidermal protoplasts using the solutions described in Materials and Methods. The pipette solution contained 5 mM Mg-ATP and 5 mM GTP. (*A*) Effect of 0.5 mM niflumic acid on the *I-V* curve. The current response to a 20-sec voltage ramp between −184 and +56 mV applied to the plasma membrane is shown before (control) and 1 min after the onset of the perfusion of 0.5 mM NA. (*B*) Time course of the effect of niflumic acid on the whole-cell current. The current at the peak potential (−100 mV) was measured every 30 sec. The establishment of the whole-cell configuration was taken as time 0. After 8 min the anion current was nearly stabilized and 0.1 mM 9-AC was injected in the external medium. After 12 min, the local perfusion containing 0.1 mM NA began. In this experiment NA inhibited 61% of the voltage-dependent anion current and its effect was fully reversible. Dose-response curves of the inhibition (*C*) and the shift (*D*) induced by niflumic acid on the voltage-dependent anion current. The maximal current and the peak potential were measured from voltage ramps before and during the local perfusion of various concentrations of NA. The symbols represent the mean ± SD of 3 to 4 experiments on different protoplasts. The lines correspond to the fitted curves obeying to the equation: $E = (E_{max} \cdot [NA])/(K + [NA])$ where E stands for inhibition/shift, [NA] for the concentration of niflumic acid, E_{max} for the maximal inhibition/shift and K for the apparent affinity. K and E_{max} were the adjustable parameters. The fit yielded K values of 83 μM and 0.43 mM and E_{max} values of 97% and −31 mV for the inhibition and the shift, respectively.

As shown in Fig. 1*C* and *D*, both effects of niflumic acid, i.e., current inhibition and peak shift were concentration-dependent. Niflumic acid inhibited the voltage-dependent anion current with an IC_{50} of 83 μM and complete inhibition could be obtained with 1 mM. As already noticed by Marten et al. (1992), the EC_{50} for the gate shifting effect was lower than the IC_{50} for the inhibition. Indeed, the fitting of the data points with a Michaelian equation gave an estimation of 430 μM for the apparent affinity and predicts a maximum shift of −31 mV.

NPPB reduced the peak amplitude by 24 ± 5% (n = 11) and 52 ± 7% (n = 4) when applied at 30 μM and 100 μM, respectively and also provoked a significant shift of the peak potential of −7 ± 2 mV at the concentration of 100 μM. Higher concentrations could not be assayed due to insolubility of the molecule in 1% ethanol in our conditions. The inhibition occurred immediately upon NPPB application and the reversibility could be observed in some cases but as it was slow (1–2 min), it often overlapped with the rundown of the anion current. IAA-94 also induced inhibition of the voltage-dependent anion channel. However, 100 μM and 500 μM IAA-94 induced an inhibition of the anion current of 26 ± 6% (n = 3) and 29 ± 4% (n = 3), respectively, and induced the same shift of −4 ± mV (*data not shown*). This suggest that IAA-94 is not able to block completely the voltage-dependent anion current but that it interacts with the channel with an affinity below 100 μM. As observed

with niflumic acid the effect of IAA-94 was rapid and reversible.

The Nucleotide Regulation of the Hypocotyl Anion Channel Does Not Require ATP Hydrolysis

The hypocotyl anion channel has been previously shown to be regulated by ATP (Thomine et al., 1995). However, the question whether ATP acted as a donor of phosphate group or by binding at a nucleotide regulatory site remained. To address this question we compared the effect of AMPPNP, a nonhydrolyzable structural analogue of ATP, with that of Mg-ATP on the anion current. The cytoplasm of the protoplast was perfused by a pipette solution containing either Mg-ATP or AMPPNP in the whole-cell configuration. In these conditions, the anion current activated to an amplitude and a peak potential characteristic of the nucleotide concentration in the pipette and then began to rundown. Measurements were done just before the onset of rundown.

Figure 2 shows representative results obtained with various concentrations of Mg-ATP or AMPPNP in the pipette. With a pipette containing 0.1 mM Mg-ATP or AMPPNP, depolarizing pulses from a resting potential of −184 to −134 mV induced the activation of the inward current with time constants of 32 ± 10 msec ($n = 5$) and 23 ± 13 msec ($n = 4$) for Mg-ATP and AMPPNP respectively (Fig. 2*A* and *B*). Depolarization to −94 mV elicited smaller currents with faster activation kinetics of 2.3 ± 0.9 msec (Mg-ATP, $n = 4$, Fig. 2*A*) and 2.9 ± 1.5 msec (AMPPNP, $n = 4$, Fig. 2*B*). This corresponded to anion currents activating at hyperpolarized threshold (around −160 mV) and reaching a maximal amplitude at potentials of −134 ± 7 mV (Mg-ATP, $n = 6$, Fig. 2*E*) and −126 ± 8 mV (AMPPNP, $n = 5$, Fig. 2*F*). These very negative peak potentials were similar to the one observed using a pipette lacking nucleotides (Thomine et al., 1995).

Figure 2*C* and *D* show the currents elicited by depolarizing pulses when the concentration of Mg-ATP or AMPPNP was raised to 10 mM. In these conditions, depolarization to −134 mV was not sufficient to activate the current, but depolarization to −94 mV still induced the activation of the anion current with fast kinetics. The time constants for activation were 1.2 ± 0.3 msec (Mg-ATP, $n = 6$) and 0.6 ± 0.3 msec (AMPPNP, $n = 3$). This corresponded to anion currents activating at a depolarized threshold of around −120 mV and reaching peak amplitudes at −97 ± 4 mV (Mg-ATP, $n = 6$, Fig. 2*E*) and −91 ± 4 mV (AMPPNP, $n = 7$, Fig. 2*F*). Raising the nucleotide concentration from 0.1 to 10 mM reduced the maximal amplitude from −45 ± 23 μA/cm^2 ($n = 6$) to −24 ± 10 μA/cm^2 ($n = 6$) for Mg-ATP and from −50 ± 23 μA/cm^2 ($n = 5$) to −15 ± 7 μA/cm^2 ($n = 7$) for AMPPNP. Additionally, Fig 2*E* and *F* show that this effect was concentration-dependent, as intermediate inhibitions of the current and intermediate shifts of the peak potential were obtained when the inside of the cell was perfused with an intermediate concentration of 1 mM Mg-ATP or AMPPNP. Thus, AMPPNP was able to mimick the effect of Mg-ATP on the anion current, inducing similar inhibition and shift of the peak potential when tested at the same concentrations as Mg-ATP. The ability of AMPPNP, a nonhydrolyzable analogue of ATP (Young, 1975), to mimick the effect of Mg-ATP demonstrates that ATP hydrolysis is not required for channel regulation.

Furthermore, ATPγS, another nonhydrolyzable analogue of ATP, was even more efficient than Mg-ATP itself to regulate the channel. Figure 3*B* shows a comparison between the effects of Mg-ATP and ATPγS. In the presence of 5 mM Mg-ATP, the current showed a peak potential of −104 ± 5 mV and a mean maximal current density of −25 ± 5 μA/cm^2 ($n = 5$), whereas ATPγS, at the same concentration induced an extreme shift of the peak potential to −49 ± 3 mV ($n = 3$) associated with a drastic reduction of the current to −3.8 ± 1.0 μA/cm^2 ($n = 3$, Fig. 3*B*). In addition, even a concentration of only 0.25 mM ATPγS induced a more pronounced effect than 5 mM Mg-ATP, shifting the peak potential to −75 ± 1 mV and reducing the current to −12 ± 2 μA/cm^2 ($n = 4$). This finding reinforced the idea that the regulation of the voltage dependent anion channel by ATP does not require ATP hydrolysis.

However, the regulation of the channel by ATPγS had some distinctive features when compared with the effects of Mg-ATP. The shift of the peak potential by Mg-ATP was associated with a fast activation kinetics of the current at the peak potential. Figure 3*A* shows that 0.25 mM ATPγS induced a more complex kinetic behaviour. The current elicited by a depolarizing pulse to −84 mV displayed a fast component with a time constant of 2.1 ± 0.6 msec comparable to the activation in presence of ATP at a similar potential (Fig. 2*A* and *C*). But this fast component accounted only for 30 ± 10% of the current, and an additional slower component with a time constant of 22 ± 4 msec ($n = 3$) accounting for 70 ± 9% of the current was observed only in the presence of ATPγS. In addition, when a depolarizing step to −104 mV was applied to the membrane, the activation of the current was followed by a partial inactivation of 27 ± 5% ($n = 3$) of the current.

The Nucleotides Mainly Act by Shifting the Voltage Gate of the Voltage-Dependent Anion Channel

The nucleotides induce a shift of the threshold of activation of the anion channel associated with a shift of the potential for which the current reaches its maximal am-

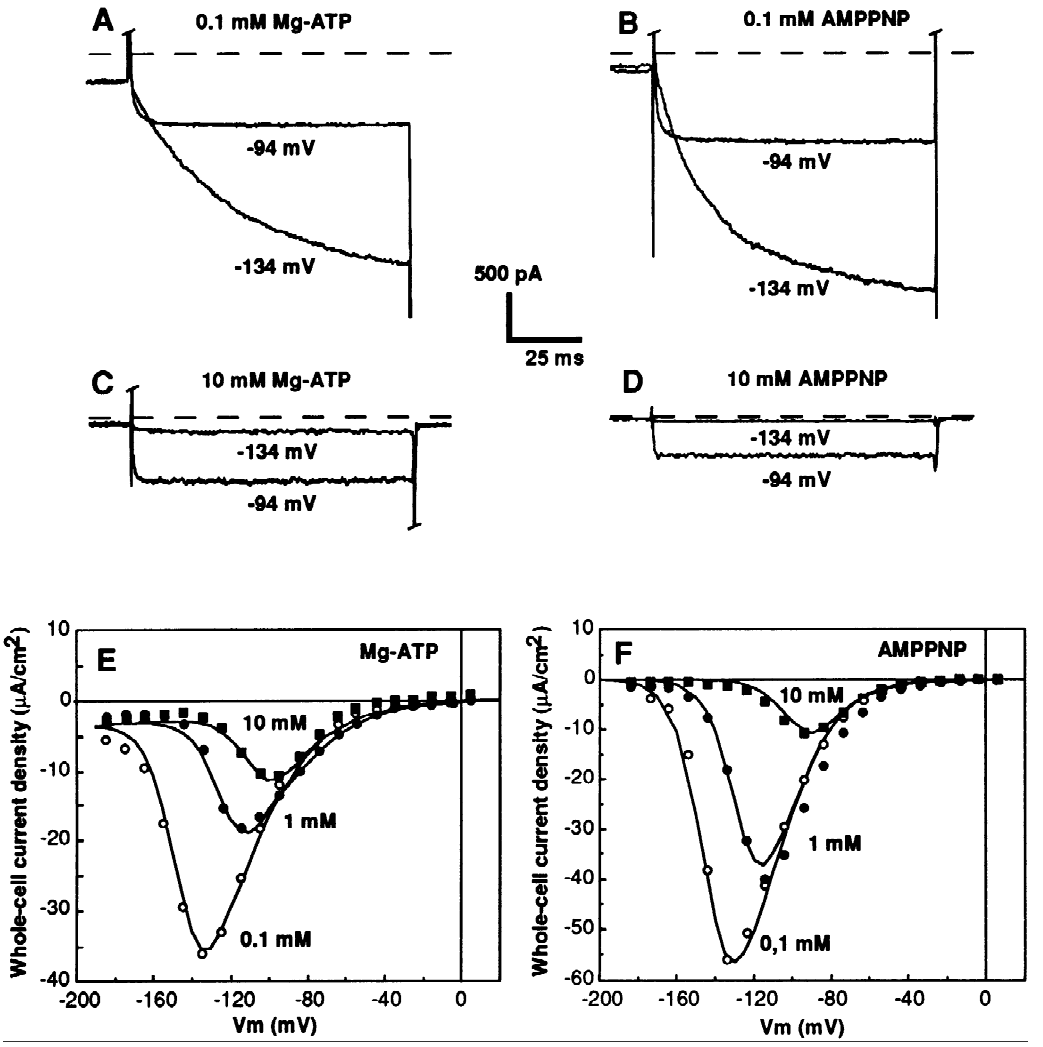

Fig. 2. Comparison between the effects of intracellular Mg-ATP and of its nonhydrolyzable analogue AMPPNP. Currents elicited by depolarizing pulses from a holding potential of −184 to −134 mV and −94 mV after perfusion of the cytosol with pipette solutions containing (in mM): 0.1 Mg-ATP (*A*), 0.1 AMPPNP (*B*), 10 Mg-ATP (*C*) or 10 AMPPNP (*D*). The dashed lines indicate the position of 0 current. The very fast capacitive transients occurring at the beginning of the pulses have been masked for the sake of clarity. Representative *I-V* curves from protoplasts perfused with either 0.1 mM (open circles), 1 mM (filled circles) or 10 mM (filled squares) Mg-ATP (*E*) or the same concentrations of AMPPNP (*F*) were constructed from the currents measured at the end of 100-msec voltage pulses to potentials ranging from −184 to +6 mV with a 10-mV increment. The currents are expressed as whole-cell current density assuming that the membrane capacity is 1 $\mu F/cm^2$. The solid lines in *E* and *F* represent *I-V* curves calculated using the model described in Materials and Methods. The parameters used to fit the data obtained with 0.1 mM Mg-ATP were: gating charge $z_g = -3.4$, potential of half activation $V_{1/2} = -145$ mV for the voltage-dependent open probability, and $z'_g = 1.5$; $V'_{1/2} = -105$ mV for the rectification of the current between the peak potential and 0 mV. Concentrations: $[Cl]_i = 162$ mM, $[Cl]_e = 110$ mM. The curves fitting the data obtained with 1 and 10 mM Mg-ATP were calculated using the same parameters except that $V_{1/2}$ was shifted from −145 to −120 mV (1 mM) and −104 mV (10 mM). The data in *F* were fitted using the same procedure, in this case, the $V_{1/2}$ values were −144 mV (0.1 mM AMPPNP), −126 mV (1 mM) and −94 mV (10 mM).

plitude (peak potential) and a reduction of the amplitude of the current. In an attempt to analyze the effect of nucleotides on the voltage-dependence of the anion channel in more detail, we used a two-pulse protocol that allowed a determination of the relative open probability of the channel at different membrane potentials (*see* Material and Methods). Figure 4*A* displays the variation of the relative open probability of the channel, as a function of the membrane potential with pipette solutions containing 0.1, 1 or 10 mM Mg-ATP. This analysis reveals that Mg-ATP induced a shift of the activation curve toward depolarized potentials. The fit of these data using the Boltzmann equation showed that, whereas the gating charge that accounts for the steepness of the voltage-dependence was nearly unchanged when the internal concentration of Mg-ATP was raised (2.8, 3.0 and 2.6 for

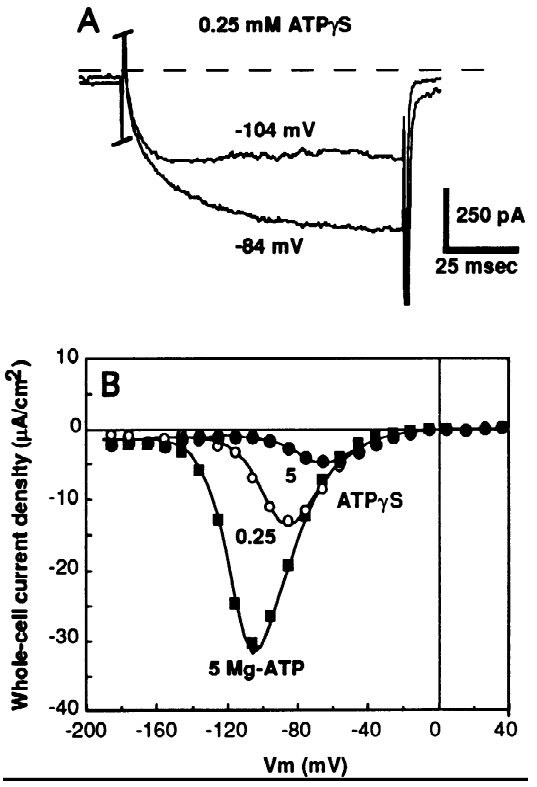

Fig. 3. Comparison between the effects of intracellular Mg-ATP and of its thiophosphate analogue ATPγS. (*A*) Currents elicited by depolarizing pulses from a holding potential of −184 to −104 and −84 mV after perfusion of the cytosol with a pipette solution containing 0.25 mM ATPγS. The dashed lines indicate the position of zero current. The very fast capacitive transients occurring at the beginning of the pulses have been masked for the sake of clarity. (*B*) Representative *I-V* curves from protoplasts perfused either with 5 mM Mg-ATP (filled squares) or with 0.25 mM (open circles) and 5 mM ATPγS (filled circles) were constructed from the currents measured at the end of 100-msec voltage pulses to potentials ranging from −184 to +6 mV with a 10-mV increment. The currents are expressed as whole-cell current density to eliminate the differences in currents amplitudes due to the different sizes of the protoplasts. The solid lines in *B* represent *I-V* curves calculated using the model described in Materials and Methods. The parameters used to fit the data obtained with 5 mM Mg-ATP were: gating charge $z_g = -3.4$, potential of half activation $V_{1/2} = -111$ mV for the voltage-dependent open probability, and $z'_g = 1.5$; $V'_{1/2} = -105$ mV for the rectification of the current between the peak potential and 0 mV. Concentrations: $[Cl]_i = 162$ mM, $[Cl]_e = 110$ mM. The curves fitting the data obtained with 0.25 mM and 5 mM ATPγS were calculated using the same parameters except that $V_{1/2}$ was shifted from −111 mV to −90 mV (0.25 mM) and −68 mV (5 mM).

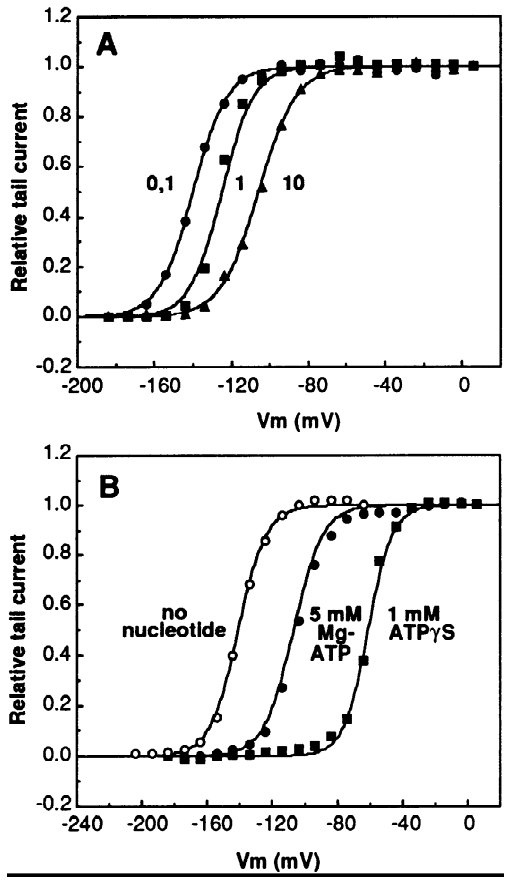

Fig. 4. Effects of nucleotides on the voltage gate of the anion channel. Tail currents were measured using a two pulse protocol as described in Materials and Methods. The tail currents were normalized and displayed as a function of the prepulse potential. The normalized data (symbols) have been fitted by Boltzmann functions. Variations of the open probability as a function of the membrane potential in protoplasts perfused with an internal solution containing 0.1, 1 or 10 mM Mg-ATP (*A*) or with an internal solution containing no nucleotide, 5 mM Mg-ATP or 1 mM ATPγS (*B*). The parameters of the Boltzmann curve were: z_g of 2.8, 3.0 and 2.5 and $V_{1/2}$ of −140, −125 and −106 mV for 0.1, 1 and 10 mM Mg-ATP, respectively (*A*), and z_g of 2.9, 2.8 and 3.3 and $V_{1/2}$ of −141, −107 and −61 mV for 0 nucleotide, 5 mM ATP and 1 mM ATPγS, respectively (*B*).

0.1, 1 and 10 mM Mg-ATP, respectively), the half activation potential ($V_{1/2}$) was shifted to depolarized values (−140, −125 and −106 mV for 0.1, 1 and 10 Mg-ATP, respectively). Figure 4*B* shows that ATPγS also acted by shifting the voltage gate of the anion channel. It also illustrates the fact that the channel can be modulated on a wide potential scale since $V_{1/2}$ can vary between −141 mV when no nucleotide is added in the internal medium and −61 mV in the presence of 1 mM ATPγS, which corresponds to a shift of 80 mV. A concentration of 5 mM Mg-ATP, close to the physiological conditions, sets the voltage gate of the channel near the middle of this range with a $V_{1/2}$ of −107 mV (Fig. 4*B*).

To show that the nucleotide-induced shift of the voltage gate accounts for all the effects of nucleotides on the *I-V* relationship of the current, the experimental data in Figs. 2*E, F* and 3*B* have been fitted using the model described in Materials and Methods. The solid lines in these figures represents the calculated *I-V* curves. In Fig. 2*E*, for example, the parameters of the model were chosen to obtain an *I-V* curve fitting the data obtained using

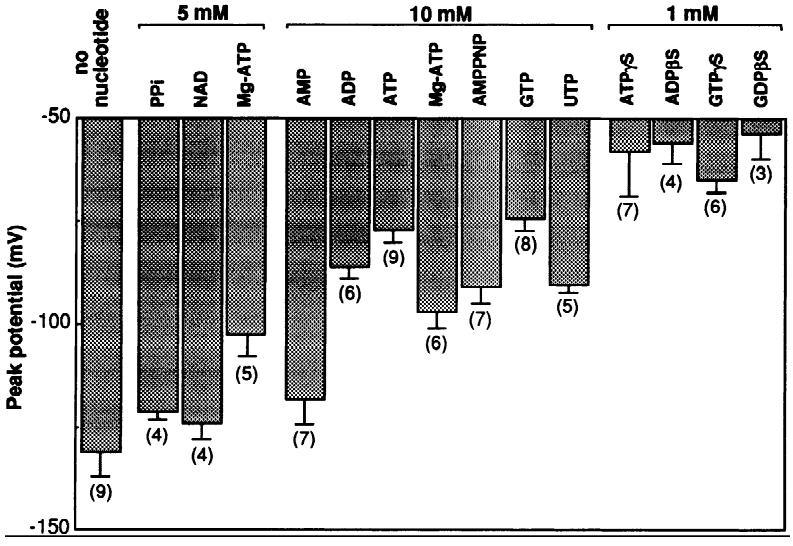

Fig. 5. Nucleotide specificity of the regulation of the voltage-dependent anion channel. Peak potentials were measured from 20-sec voltage ramps after perfusion with internal solutions containing various nucleotides, just before the onset of rundown. Mean values ± SD are shown and the numbers in parenthesis indicate the number of protoplasts tested in each condition. Except for ATP, GTP and UTP, the experiments were done using the solutions as described in Materials and Methods. In the case of ATP, GTP and UTP, the internal solution did not contain Mg^{2+}.

the 0.1 mM Mg-ATP pipette solution. The open probability has been calculated using the Boltzmann equation with a gating charge (z_g) of 3.4, and a potential of half activation ($V_{1/2}$) of −145 mV. The curves fitting the data obtained with 1 and 10 mM Mg-ATP have been generated using the same parameters with the only difference that $V_{1/2}$ has been shifted from −145 to −120 mV (1 mM) and −107 mV (10 mM). This sole modification of the position of the voltage gate was sufficient to mimick the effects of the Mg-ATP on the threshold of activation, the peak potential and the amplitude of the current at the peak. A similar procedure was applied to the data in Figs. 2*F* and 3*B* confirming that the nucleotide effect on the voltage gate is responsible for all the modifications of the *I-V* curve when intracellular nucleotide concentration is increased. Especially, the shift of the peak potential toward potentials at which the electrochemical gradient is reduced appears sufficient to account for the nucleotide-induced inhibition of the anion current. Furthermore, the strong decrease of the anion conductance at depolarized potential makes the shifts of the voltage gate most efficient to modulate the amplitude of the current at the peak potential in the range between −140 and −60 mV.

Structural Requirements for Nucleotide Activity on the Anion Current

We investigated the structural requirements for nucleotide activity on the anion current. As the most reproducible effect of nucleotides on the channel is a shift of the voltage gate that can be easily measured as a shift of the peak potential, we measured the peak values obtained at a given concentration of a range of nucleotides (Fig. 5). The following properties required for a molecule to be a channel effector can be derived from the results presented in Fig. 5: (i) Only molecules with a nucleotide structure are active, as 5 mM pyrophosphate is inactive in comparison with 5 mM Mg-ATP. The fact that 5 mM NAD which includes an ADP moiety linked with nicotinic acid in γ is inactive shows that the last phosphate group needs to be free. (ii) The number of phosphate groups as well as the nature of the bond between the groups are critical: 10 mM AMP is nearly ineffective to shift the peak potential, whereas ADP is active but not as much as ATP. Alteration of one phosphate group by substitution of an oxygen atom by a sulfur atom increases very much the activity of a given nucleotide: 1 mM ATPγS, ADPβS, GTPγS or GDPβS are more efficient than a ten times higher concentration of ATP or GTP. The presence of an *N* bond between two phosphate groups diminishes the activity: AMPPNP is less efficient than free ATP. (iii) The nature of the base is not critical: 10 mM ATP, 10 mM GTP or 10 mM UTP induce a similar shift of the peak potential and ATPγS and GTPγS display similar activity. These requirements define the profile of the nucleotide binding site involved in the regulation of the hypocotyl anion channel.

We studied the activity of some selected nucleotides in more detail by establishing their dose-response curves (Fig. 6). The data were fitted with a Michaelian equation assuming a single binding site for nucleotides, although a clear saturation was not reached for every nucleotide. This allowed the determination of two parameters that are important for the regulation: the apparent affinity of the binding site for a nucleotide and the maximal shift of the peak potential that a nucleotide can induce. Figure 6*A* recapitulates the dose-response curves to Mg-ATP and its two nonhydrolyzable analogues AMPPNP and ATPγS that were presented in the first part of the results (Figs. 2 and 3). As already underlined, Mg-ATP and AMPPNP were similarly effective. A Michaelian fit of

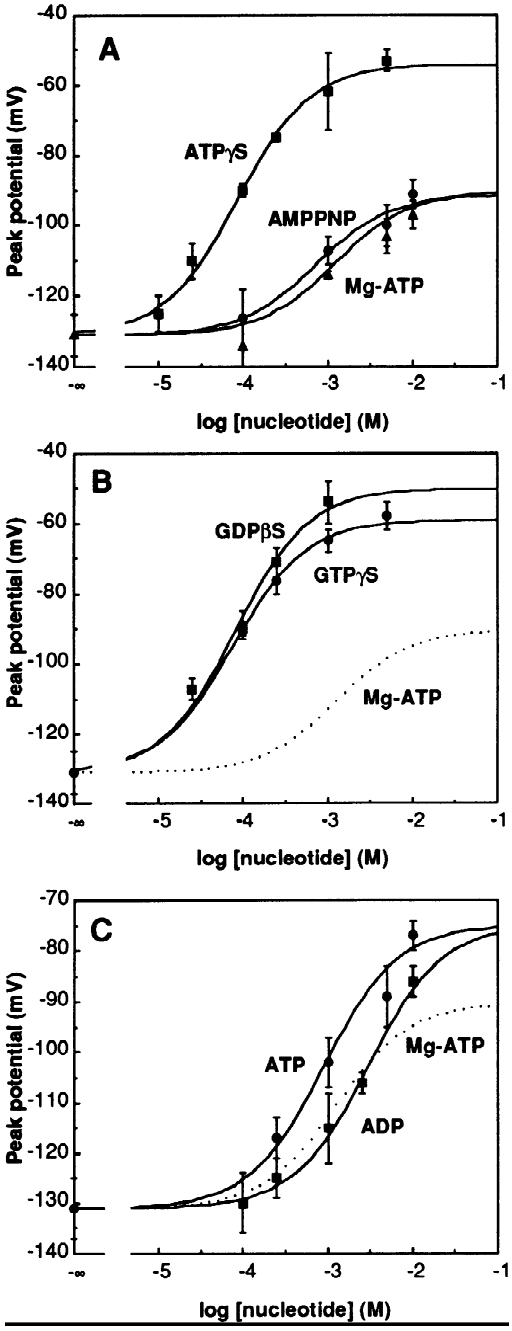

Fig. 6. Concentration-dependent effects of nucleotides. The peak potentials were measured from 20-sec voltage ramps after perfusion with internal solutions containing various concentrations of different nucleotides, just before the onset of rundown. The data points represent the means of these measurements ± SD. The curves represent the fit of the data by the following equation describing the fixation of an agonist on a single binding site:

$$V_{peak} = V_{peak(0)} + (\Delta V_{peak(max)} \cdot [N])/(K + [N])$$

where V_{peak} stands for peak potential, [N] for the concentration of nucleotide, $V_{peak(0)}$ for the peak potential in the absence of intracellular nucleotides, $\Delta V_{peak(max)}$ for the maximal shift of the peak potential and K for the apparent affinity. The adjustable parameters were K and $\Delta V_{peak(max)}$. (*A*) Comparison between the dose response curves for Mg-ATP and two nonhydrolyzable analogues, AMPPNP and ATPγS. The number of protoplasts tested was 9 in the absence of nucleotide, and 5–7, 5–7 and 3–7 for the various concentrations of Mg-ATP, AMPPNP and ATPγS, respectively. The data were fitted with K values of 1.2 mM, 0.7 mM and 86 μM, and $\Delta V_{peak(max)}$ values of 41, 40 and 77 mV for Mg-ATP, AMPPNP and ATPγS, respectively. (*B*) Effects of thiophosphate analogues of guanine nucleotides. The dashed curve corresponds to the fit obtained for Mg-ATP given as a reference. The number of protoplasts tested were 4–6 and 3–9 for the various concentrations of ATPγS and GDPβS, respectively. The data were fitted with K values of 75 μM and 81 μM, and ΔVpeak(max) values of 73 mV, and 81 mV for GTPγS and GDPβS, respectively. (*C*) Comparison between the dose-response curves for ATP and ADP. Note that ADP was tested in the presence of 2 mM of Mg^{2+}, whereas ATP was tested in the absence of intracellular Mg^{2+}. As in *B*, the dashed curve corresponds to the fit obtained for Mg-ATP given as a reference. The number of protoplasts tested were 7–9 (except 0.25 mM, $n = 2$) and 4–6 for the various concentrations of ATP and ADP, respectively. The data were fitted with K values of 0.9 and 2.9, and $\Delta V_{peak(max)}$ values of 56, and 58 mV for ATP and ADP, respectively.

the experimental data yields similar apparent affinities for the regulatory site with EC_{50} of 1.2 and 0.7 mM, and similar maximal shifts of +41 and +40 mV, for Mg-ATP and AMPPNP, respectively. In contrast, ATPγS is much more potent than Mg-ATP and AMPPNP. It shows a higher apparent affinity for the nucleotide binding site with an EC_{50} of 86 μM and also a greater maximal shift of +77 mV. This shows that even moderate modifications of the structure of the nucleotide can modify both their affinity for the site and the maximal response they are able to induce. We also analyzed the response to GTPγS and GDPβS (Fig. 6*B*). Their properties are very close to those of ATPγS. They display EC_{50} of 75 and 81 μM and induce maximal shifts of +75 and +81 mV, respectively.

Nucleotide regulations are classically interpreted as a way to couple the activity of a protein and the energetic status of the cell. Thus it was important to clarify the difference between the effects of ATP, Mg-ATP, ADP and AMP. Figure 6*C* shows the dose-response curves for ATP, ADP and Mg-ATP (dashed line, *see* Fig. 6*A*). The comparison between the dose-response curves for ATP and Mg-ATP reveals that Mg^{2+} diminishes the efficiency of ATP mainly by decreasing the maximal shift of the peak potential from +55 to +40 mV whereas the EC_{50} of the nucleotide is only slightly increased from 0.9 mM for ATP to 1.2 mM for Mg-ATP. The comparison between the dose-response curves for ADP and ATP shows that ATP has a 3-fold greater apparent affinity than ADP ($EC_{50} = 2.9$ mM) but the maximal shifts they can induce are similar.

Discussion

In this work we show that the voltage-dependent anion channel of *Arabidopsis* hypocotyls displays original properties in terms of sensitivity to anion channel blockers and nucleotide-dependent regulation.

Pharmacological Properties

Although the identity of this channel as an anion channel has been demonstrated previously (Thomine et al., 1995), it lacks sensitivity to some of the most common anion channel blockers. 9-AC and DIDS, which have been shown to be potent inhibitors of chloride channels in many animal cell types (Greger, 1990; Paulmichl et al., 1993) and of plant voltage-dependent anion channels (Marten et al., 1992, 1993; Schwartz et al., 1995; Zimmermann et al., 1994) had no effect on the voltage-dependent anion channel of hypocotyl cells. Among the active inhibitors, none was found to interact with the channel with an affinity as high as those found for guard cell anion channels (Marten et al., 1992, 1993; Schroeder et al., 1993). IAA-94, which was developed to purify chloride channels from kidney and trachea (Landry et al., 1989) and which blocks both rapid and slow anion channel in guard cells with IC_{50} below 10 μM, inhibited only 29% of the hypocotyl anion current at the concentration of 500 μM. Similarly, NPPB at 100 μM inhibited only 50% of the voltage-dependent anion current of *Arabidopsis* hypocotyl cells whereas it blocks both S-type and R-type anion currents of guard cells, as well as the blue light activated anion channel of *Arabidopsis* hypocotyl cells with IC_{50} below 10 μM. Niflumic acid is the most efficient blocker that we identified to date. It induced both an inhibition of the current and a shift of the voltage gate of the anion channel toward hyperpolarized potentials, which is comparable to the effect of different blockers on guard cell anion channels of the rapid type (Marten et al., 1992). Altogether, these properties define an original pharmacological profile for the voltage-dependent anion channel of *Arabidopsis* hypocotyls. It is of interest that this pharmacological profile allows to distinguish between this channel and the blue light activated anion channel of *Arabidopsis* hypocotyls that is sensitive to micromolar concentrations of NPPB. However, both niflumic acid and NPPB have been shown not to be specific for anion channels as they efficiently inhibit outward potassium currents in wheat root protoplasts (Garill et al., 1996). To help for the determination of the physiological role of the voltage-dependent anion channel in the plant, the pharmacological data presented here need to be completed by the identification of high affinity specific antagonists.

Nucleotide Regulation

In this study, we could confirm that, as found in our initial characterization of the hypocotyl voltage-dependent anion channel (Thomine et al., 1995), nucleotides accelerate the deactivation kinetics at a given membrane potential, although this effect has not been studied further (*data not shown*). We also show that the activation kinetics of the channel is accelerated by depolarization but that ATP does not alter significantly the activation kinetics at −94 mV (2.3 ± 0.9 msec and 1.2 ± 0.3 msec with 0.1 mM and 10 mM internal Mg-ATP, respectively). The results presented focus on new insights into the regulation of this channel by ATP. Several lines of arguments demonstrate that ATP hydrolysis is not required for the regulation: (i) Nonhydrolyzable analogues of ATP, AMPPNP and ATPγS, are as efficient or more efficient than Mg-ATP to induce the shift of the voltage gate. (ii) ATP is more efficient in the absence of Mg^{2+} than Mg-ATP complex to induce the shift, although Mg-ATP is the proper substrate for hydrolysis. (iii) ADP and other dinucleotides, ADPβS and GDPβS, induce significant shifts of the peak potential, although they cannot be substrates for kinases. Thus, the regulation of this channel by ATP reflects the binding of the nucleotide on a regulatory site rather than its use as a substrate for kinase or energy-dependent processes. Thiophosphate nucleotide analogues display a striking efficiency to regulate the channel and therefore appear as extremely potent agonists for the nucleotide receptor involved. The guanyl nucleotides, GTPγS and GDPβS, were the first thionucleotides that we tested. We have been confused by their striking efficiencies and believed for some time that a G-protein regulation was involved. This points to the importance of making ATPγS controls when studying a regulation by G-proteins.

The structural requirements for the regulatory effect on *Arabidopsis* anion channel match closely those that have been described for K_{ATP} channels of some animal cell types (Ashcroft, 1988). A sequence of efficiency ATP > ADP ⩾ AMP, similar to what we found, has been described for K_{ATP} channels of frog skeletal muscle and of guinea pig ventricular cells (Kakei, Noma & Shibasaki, 1985; Spruce, Standen & Stanfield, 1987). In particular, K_{ATP} from frog skeletal muscles have a 3 times higher affinity for ATP than for ADP (Spruce et al., 1987) which is exactly what we found for the hypocotyl anion channel. Based on the decrease of ATP efficiency by Mg^{2+} and on a comparison between the pKa of the various nucleotides and their relative efficiencies, it has been proposed that the charge carried by the phosphate groups of the nucleotides might be an important determinant of their capacity to inhibit K_{ATP} in rat pancreatic β-cells (Ashcroft & Kakei, 1989). The hypothesis of a similar determination of nucleotide efficiency for the hypocotyl anion channel is supported by the fact that Mg^{2+} decreased ATP efficiency and also by the high potency of thiophosphate analogues that have lower pKa than ATP (7 for ATP and 5.8 for ATPγS) and thus carry

a higher charge at physiological pH. Additional features of the nucleotides, such as their spatial organization, must also be involved in the determination of their efficiency.

The regulation of the anion channel by nucleotides also displays some properties distinct from those described for K_{ATP} channels. First, the affinity of K_{ATP} channel for ATP (EC_{50} in the range of 100 μM; Ashcroft, 1988) is ten times higher than the one we found for the voltage-dependent anion channel. Second, GTP was found to be ineffective or ten times less effective than ATP to inhibit K_{ATP} (Ashcroft, 1988), whereas we found similar efficiency for ATP and GTP. Third, a major distinctive feature of the regulation of the anion channel by nucleotides is the high potency of thiophosphate nucleotide analogues.

Regulations by nucleotides have also been described for other plant ion channels. Spalding & Goldsmith (1993) characterized a potassium channel that is activated by ATP produced photosynthetically, but whether ATP needs to be hydrolyzed to produce its effect was not addressed. The guard cell R-type anion channel is also regulated by nucleotides (Hedrich et al., 1990; Schulz-Lessdorf et al., 1996). In this case, AMPPNP, ATPγS, GTPγS can replace ATP to activate the channel demonstrating that the regulation likely involves a nucleotide binding site. Both this regulation and the one described here concern voltage-dependent anion channels but nucleotides have opposite effects on the guard cell anion channel and on the hypocotyl epidermal cell anion channel. In the first case, they are required to support the calcium dependent activation of the channel (Hedrich et al., 1990) whereas in the second they exert an inhibitory effect on the current.

We show that the nucleotides induce a shift of the voltage gate of the hypocotyl anion channel. We argue that this effect can account for all the modifications that ATP induces on the current. Indeed, modeling the effect of the sole change of the half activation potential on the *I-V* curve of the anionic current mimicks both the change in voltage regulation and the diminution of the maximal current amplitude induced by ATP. Thus, the nucleotides inhibit the anion current by shifting the voltage gate of the channel. This regulation mechanism is very efficient because it does not only reduce the maximal intensity of the current but also sends the threshold for activation away from the resting potential of hypocotyl cells (Spalding & Cosgrove, 1992; Stirnberg, King & Barbier-Brygoo, 1995). This means that larger depolarizations are required to activate the voltage-dependent anion channel when it is inhibited by nucleotides. Two main hypotheses can be envisaged for the mechanism of nucleotide effect on the voltage dependence of the anion channel. One possible hypothesis would be that the channel has an intrinsic voltage-dependent gate and this gate can be modulated through an intracellular binding site for nucleotides. An alternative hypothesis would be that nucleotides themselves are responsible for the observed voltage dependence by entering a binding site located within the pore in a voltage-dependent manner and produce a voltage-dependent block of the open channel (Woodhull, 1973). Although this latter hypothesis is attractive, its assessment would require further analysis.

Relevance of the Nucleotide Regulation

We provide arguments that the regulation of the channel by nucleotides can be a mean to couple its activity with the energetic metabolism of the cell. The apparent affinity for ATP is consistent with the known intracellular concentrations of 1 to 2 mM ATP determined in cultured sycamore cells and in maize root tip cells (Gout, Bligny & Douce, 1992; Saint-Ges et al., 1991; Xia, Saglio & Roberts, 1995). When the cells are subjected to anoxic stress (Xia et al., 1995) or when the proton pump ATPase is stimulated by cytosolic acidification (Gout et al., 1992), the intracellular ATP concentration can decrease to values as low as 0.5 mM. When the ATP pool decreases, ADP does not accumulate in the cytosol (Gout et al., 1992; Xia et al., 1995), likely due to high dinucleotide kinase activity in plant cells. Thus, when ATP is consumed, it is rather converted to AMP (Gout et al., 1992; Xia et al., 1995). As AMP is nearly inactive to modulate the anion current (Fig. 5), a drop in the ATP level will result in a large shift of the voltage gate of the channel. Furthermore, the nucleotide concentrations that occur in the neighborhood of the plasma membrane may undergo even larger variations. Indeed, the plant plasma membrane carries the ATPase proton pump which is one of the greatest ATP consumer of the cell. It also has to be considered that shifts of the gate in the voltage range concerned have strong effects on the current amplitude due to the rectifying properties of the current *I-V* curve. Thus the nucleotide regulation that we describe can potentially couple the anion channel activity with the energetic metabolism of the cell and it is tempting to speculate that the nucleotide regulation of the anion channels could be a mean to couple their activity with that of the proton pump ATPase. They would be activated when the consumption of ATP by the ATPase overcomes the capacity of the cell machinery to generate enough ATP.

This research was supported by the European Community's BIOTECH program, as a part of the Project of Technological Priority 1993–1996 and by the CNRS (UPR0040). S. Thomine was funded by the Ministère de l'Enseignement Supérieur et de la Recherche.

References

Ashcroft, F.M. 1988. Adenosine-5′-triphosphate-sensitive potassium channels. *Ann. Rev. Neurosci.* **11:**97–118

Ashcroft, F.M., Kakei, M. 1989. ATP-sensitive K^+ channels in rat pancreatic β-cells: modulation by ATP and Mg^{2+} ions. *J. Physiol.* **416:**349–367

Cho, M.H., Spalding, E.P. 1996. An anion channel in *Arabidopsis* hypocotyls activated by blue light. *Proc. Natl. Acad. Sci. USA* **93:**8134–8138

Ebel, J., Cosio, E.G. 1994. Elicitors of plant defense responses. *Int. Rev. Cyt.* **148:**1–36

Elzenga, J.T.M. 1991. Patch clamping protoplasts from vascular plants. *Plant Physiol.* **97:**1573–1575

Garrill, A., Tyerman, S.D., Findlay, G.P., Ryan, P.R. 1996. Effects of NPPB and niflumic acid on outward K^+ and Cl^- currents across the plasma membrane of wheat root protoplasts. *Aust. J. Plant Physiol.* **23:**527–534

Gout, E., Bligny, R., Douce, R. 1992. Regulation of intracellular pH values in higher plant cells. *J. Biol. Chem.* **267:**13903–13909

Greger, R. 1990 Chloride channel blockers. *Methods in Enzymology* **191:**793–809

Hamill, O.P., Marty, A., Neher, E., Sakmann, B., Sigworth, F.J. 1981. Improved patch-clamp techniques for high-resolution current recording from cells and cell-free membrane patches. *Pfluegers Arch.* **391:**85–100

Hedrich, R., Busch, H., Raschke, K. 1990. Ca^{2+} and nucleotide dependent regulation of voltage dependent anion channels in the plasma membrane of guard cells. *EMBO J.* **9:**3889–3892

Hedrich, R., Marten, I. 1993. Malate induced feedback regulation of plasma membrane anion channels could provide CO_2 sensor to guard cells. *EMBO J.* **12:**897–901

Hille, B. 1992. Ionic Channels of Excitable Membranes. Second edition, Sinauer Associates, Sunderland, MA

Kakei, M., Noma, A., Shibasaki, T. 1985. Properties of adenosine-triphosphate-regulated potassium channels in guinea-pig ventricular cells. *J. Physiol* **363:**441–462

Landry, D.W., Akabas, M.H., Redhead, C., Edelman, A., Cragoe, E.J., Al-Awqati, Q. 1989. Purification and reconstitution of chloride channels from kidney and trachea. *Science* **244:**1469–1472

Marten, I., Busch, H., Raschke, K., Hedrich, R. 1993. Modulation and block of the plasma membrane anion channel of guard cells by stilbene derivatives. *Eur. Biophys. J.* **21:**403–408

Marten, I., Lohse, G., Hedrich, R. 1991. Plant growth hormones control voltage-dependent activity of anion channels in plasma membrane of guard cells. *Nature* **353:**758–762

Marten, I., Zeilinger, C., Redhead, C., Landry, D.W., Al-Awqati, Q., Hedrich, R. 1992. Identification of a voltage-dependent anion channel in the plasma membrane of guard cells by high-affinity ligands. *EMBO J.* **11:**3569–3575

Murashige, T., Skoog, F. 1962. A revised medium for rapid growth and bioassays with tobacco tissues cultures. *Physiol. Plant* **15:**473–497

Neher, E. 1992. Correction for liquid junction potentials in patch-clamp experiments. *Methods Enzymol.* **207:**123–131

Paulmichl, M., Gschwentner, M., Wöll, E., Schmarda, A., Ritter, M., Kanin, G., Ellemunter, H., Waitz, W., Deetjen, P. 1993. Insight into the structure-function relation of chloride channels. *Cell Physiol. Biochem.* **3:**374–387

Saint-Ges, V., Roby, C., Bligny, R., Pradet, A., Douce, R. 1991. Kinetic studies of the variations of cytoplasmic pH, nucleotides triphosphates (^{31}P-NMR) and lactate during normoxic and anoxic transitions in maize root tips. *Eur. J. Biochem.* **200:**477–482

Schmidt, C., Schelle, I., Liao, Y-J., Schroeder, J.I. 1995. Strong regulation of slow anion channels and abscisic acid signaling in guard cells by phosphorylation and dephosphorylation events. *Proc. Natl. Acad. Sci. USA* **93:**9535–9539

Schroeder, J.I., Hagiwara, S. 1989. Cytosolic calcium regulates ion channels in the plasma membrane of *Vicia faba* guard cells. *Nature* **338:**427–430

Schroeder, J.I., Schmidt, C., Sheaffer, J. 1993. Identification of high-affinity slow anion channel blockers and evidence for stomatal regulation by slow anion channels in guard cells. *Plant Cell* **5:**1831–1841

Schulz-Lessdorf, B., Lohse, G., Hedrich R. 1996. GCAC1 recognizes the pH gradient across the plasma membrane: a pH-sensitive and ATP-dependent anion channel links guard cell membrane potential to acid and energy metabolism. *Plant J.* **10**(6):993–1004

Schwartz, A., Ilan, N., Schwartz, M., Sheaffer, J., Assmann, S.M., Schroeder, J.I. 1995. Anion-channel blockers inhibit S-type anion channels and abscisic acid responses in guard cells. *Plant Physiol.* **109:**651–658

Spalding, E.P., Cosgrove, D.J. 1992. Mechanism of blue-light-induced plasma-membrane depolarization in etiolated cucumber hypocotyls. *Planta* **188:**199–205

Spalding, E.P., Goldsmith, M.H.M. 1993. Activation of K^+ channels in the plasma membrane of Arabidopsis by ATP produced photosynthetically. *Plant Cell* **5:**477–484

Spruce, A.E., Standen, N.B., Stanfield, P.R. 1987. Studies of the unitary properties of adenosine-5′-triphosphate-regulated potassium channels of frog skeletal muscle. *J. Physiol.* **382:**213–236

Stirnberg, P., King, P.J., Barbier-Brygoo, H. 1995. An auxin resistant mutant of *Nicotiana plumbaginifolia* Viv. is impaired in 1-naphtaleneacetic acid-induced hyperpolarization of hypocotyl cell membranes in intact seedlings. *Planta* **196:**706–711

Thomine, S., Zimmermann, S., Guern, J., Barbier-Brygoo, H. 1995. ATP-dependent regulation of an anion channel at the plasma membrane of epidermal cells of Arabidopsis hypocotyls. *Plant Cell* **7:**2091–2100

Tyerman, S.D. 1992. Anion channels in plants. *Annu. Rev. Plant Physiol. Plant Mol. Biol.* **43:**351–373

Ward, J.M., Pei, Z-M., Schroeder, J.I. 1995. Roles of ion channels in initiation of signal transduction in higher plants. *Plant Cell* **7:**833–844

Xia, J-H., Saglio, P., Roberts, J.K.M. 1995. Nucleotide levels do not critically determine survival of maize root tips acclimated to a low-oxygen environment. *Plant Physiol.* **108:**589–595

Woodhull, A.M. 1973. Ionic blockage of sodium channels in nerve. *J. Gen. Phys.* **61:**687–708

Yount, R.G. 1975. ATP analogs. *Advances in Enzymology* **43:**1–56

Zimmermann, S., Thomine, S., Guern, J., Barbier-Brygoo, H. 1994. An anion current at the plasma membrane of tobacco protoplasts shows ATP-dependent voltage regulation and is modulated by auxin. *Plant J.* **6:**707–716